Development 129, 4797-4806 (2002)
Printed in Great Britain © The Company of Biologists Limited 2002
DEV2915

Abnormal lymphatic vessel development in neuropilin 2 mutant mice

Li Yuan[1], Delphine Moyon[1], Luc Pardanaud[1], Christiane Bréant[1], Marika J. Karkkainen[2], Kari Alitalo[2] and Anne Eichmann[1,*]

[1]INSERM U36, Collège de France, 11, place Marcelin Berthelot, 75005 Paris, France
[2]Molecular/Cancer Biology Laboratory, Biomedicum Helsinki, 00014 Helsinki, Finland
*Author for correspondence (e-mail: anne.eichmann@college-de-france.fr)

Accepted 11 July 2002

SUMMARY

Neuropilin 2 is a receptor for class III semaphorins and for certain members of the vascular endothelial growth factor family. Targeted inactivation of the neuropilin 2 gene (*Nrp2*) has previously shown its role in neural development. We report that neuropilin 2 expression in the vascular system is restricted to veins and lymphatic vessels. Homozygous *Nrp2* mutants show absence or severe reduction of small lymphatic vessels and capillaries during development. This correlated with a reduction of DNA synthesis in the lymphatic endothelial cells of the mutants. Arteries, veins and larger, collecting lymphatic vessels developed normally, suggesting that neuropilin 2 is selectively required for the formation of small lymphatic vessels and capillaries.

Key words: Endothelial cell, Growth factor receptor, Lymphangiogenesis, Mouse

INTRODUCTION

The vertebrate vascular system is composed of arteries, veins and capillaries, and develops early in embryonic development in order to accommodate the output of the first heart beat. The lymphatic vascular system serves to transport tissue fluid, extravasated plasma proteins and cells back to the circulation (for a review, see Karkkainen et al., 2002). Lymphatic endothelial cells (EC) are thought to develop by sprouting from veins in a process referred to as lymphangiogenesis (Sabin, 1909). Mesoderm-derived lymphangioblasts may also contribute to lymphangiogenesis (Wilting et al., 2000). Recent reports have focused on the role of members of the vascular endothelial growth factor (VEGF) family in the development of arteries, veins and lymphatic vessels. VEGF is a key regulator of EC functions and is required for the formation of the primitive vascular plexus (Carmeliet et al., 1996; Ferrara et al., 1996). The VEGF family also comprises placenta growth factor (PlGF), VEGFB, VEGFC and VEGFD. The biological effects of these growth factors are mediated by binding to three EC tyrosine kinase receptors, VEGFR1-VEGFR3 (for reviews, see Neufeld et al., 1999; Veikkola et al., 2000). VEGF binds to VEGFR1 and VEGFR2, while VEGFC and VEGFD bind to VEGFR2 and are the only known ligands for VEGFR3. The expression of VEGFR3 becomes restricted to lymphatic EC from mid-gestation stages onward both in murine and in avian embryos (Kaipainen et al., 1995; Wilting et al., 1997).

Several studies have shown that VEGF signals angiogenesis, while VEGFC and VEGFD induce lymphangiogenesis. Overexpression of VEGF in the skin of transgenic mice or on the chick chorioallantoic membrane stimulates growth of blood-vascular capillaries without affecting the lymphatic vessels (Detmar et al., 1998; Wilting et al., 1996). Conversely, overexpression of VEGFC in the same mouse or chick models stimulates lymphangiogenesis with only a weak effect on blood-vascular EC (Jeltsch et al., 1997; Oh et al., 1997). Lymphangiogenesis could be selectively inhibited by overexpression of a soluble VEGFR3 (Makinen et al., 2001). VEGFC and VEGFD have also been shown to stimulate metastasis via the lymphatic vessels (Karpanen et al., 2001; Mandriota et al., 2001; Skobe et al., 2001; Stacker et al., 2001). A role for VEGFR3 as the signaling receptor mediating VEGFC or VEGFD actions was suggested by overexpression of a VEGFC form that does not bind VEGFR2 (VEGF-C156S) in the skin of mice, which also stimulates lymphangiogenesis (Veikkola et al., 2001). Moreover, mutations in the tyrosine kinase domain of VEGFR3 have been linked to human hereditary primary lymphoedema, and mice harboring an ENU-induced mutation in the kinase domain of VEGFR3 also develop lymphoedema (Karkkainen et al., 2000; Karkkainen et al., 2001).

Several members of the VEGF family have been recently shown to bind to the non-kinase neuropilin (NRP) receptors. This small family of type I transmembrane proteins includes NRP1 (NRP – Mouse Genome Informatics) and NRP2. Neuropilins were initially discovered in the nervous system, where they function as receptors for the class III family of semaphorins (Sema) to mediate chemorepulsive guidance of developing axons (Chen et al., 1997; He and Tessier-Lavigne, 1997; Kolodkin et al., 1997). NRP1 and NRP2 show overlapping sema binding specificities in vitro: NRP1 binds with high affinity to Sema3a, Sema3c and Sema3f, while NRP2 is a high affinity receptor for Sema3c and Sema3f (Chen et al., 1997; Feiner et al., 1997). However, NRP1 function appears

only necessary for Sema3a-mediated repulsive guidance events, both in vitro and in vivo, and genetic ablation of *Nrp1* phenocopies the neuronal defects observed in *Sema3a* mutant mice (Kitsukawa et al., 1997). Gene inactivation of *Nrp2* results in a distinct neuronal phenotype compared with the *Nrp1* mutation (Chen et al., 2000; Giger et al., 2000). Homozygous *Nrp2* mutants specifically lose their response to repulsive guidance events mediated by Sema3f. Fasciculation and guidance of distinct subsets of cranial nerves are perturbed in *Nrp1* and *Nrp2* mutants: $Nrp1^{-/-}$ showed deficiencies in the cranial nerves VII, IX and X, which were not affected in $Nrp2^{-/-}$ mice. Conversely, cranial nerves III and IV, which were normal in *Nrp1* mutants, showed abnormal projections in $Nrp2^{-/-}$ animals (Chen et al., 2000; Giger et al., 2000; Kitsukawa et al., 1997). Altogether, these results suggested specific, non-redundant functions for NRP1 and NRP2 in the nervous system.

Nrp1 mutant mice also showed severe defects in cardiovascular development, resulting in death of homozygous embryos by embryonic day (E) 14 (Kawasaki et al., 1999). Defects in vessel formation included failure of capillary ingrowth into the brain and abnormal formation of aortic arches and yolk-sac vasculature. These defects may be due to a requirement of NRP1 as a receptor for several members of the VEGF family, including the heparin-binding VEGF isoforms VEGF165 and VEGF145 as well as VEGFB, VEGFE and PlGF (for a review, see Neufeld et al., 2002). NRP1 enhanced VEGF165 binding to VEGFR2 and VEGFR2-mediated chemotaxis response of EC (Miao et al., 1999; Soker et al., 1998). In the developing avian vascular system, *Nrp1* showed specific expression in arterial EC (Moyon et al., 2001; Herzog et al., 2001).

NRP2 has also been shown to bind several VEGF family members, including VEGF165, VEGF145, PlGF and VEGF-C (Karkkainen et al., 2001) (reviewed by Neufeld et al., 2002). A specific role for NRP2 in the vascular system has not been described previously. Indeed, many *Nrp2* mutants are viable until adulthood and show a grossly normal cardiovascular system. We report that the formation of small lymphatic vessels and capillaries is abnormal in *Nrp2* homozygous mice. In all tissues examined, including the heart, lung, diaphragm, gut and skin, these vessels are absent or severely reduced until postnatal stages. These observations show a selective requirement of NRP2 in lymphatic vessel development.

MATERIALS AND METHODS

Mice

Nrp2 mutant mice in CD1 and C57B6 background were kindly provided by M. Tessier-Lavigne and maintained in a conventional animal facility. As previously described, $Nrp2^{+/-}$ mice appear unaffected by the mutation, while $Nrp2^{-/-}$ mice show deficiencies in the guidance and fasciculation of cranial nerves III and IV, defective development of the dorsal funiculus, absence or severe reduction of the anterior commissure and the habenular tract, and hippocampal mossy fiber projection defects (Chen et al., 2000). Adult $Nrp2^{+/-}$ mice of each genetic background were intercrossed to maintain the colony and to obtain $Nrp2^{-/-}$ animals. For RT-PCR, the procedure described by Chen et al. (Chen et al., 2000) was modified as follows: 2 bp were added on the 3′ end of primer Rc, specific primers (Rc and Rv) were used for the RT reaction and PCR was performed using ready-to-go PCR beads (Amersham Pharmacia Biotech).

In situ hybridization

In situ hybridization has been described previously (Moyon et al., 2001,) except that 6 μg/ml proteinaseK was used. Probes were a 1.2 kb mouse *Nrp2* fragment (Chen et al., 1997), a 2.2 kb rat *Nrp1* fragment (position 104-2388) (kindly provided by A. Chédotal) and a mouse *Vegfr3* fragment (position 2411-4154).

Immunohistochemistry

Tissue biopsies were fixed in 4% paraformaldehyde, dehydrated and embedded in paraffin. Immunohistochemistry was performed using the Tyramide Signal Amplification system (TSA™, NEN™ Life Science Products, Boston, MA). Peroxidase activity was developed with 3-amino-9-ethyl carbazole (Sigma). Antibodies were a monoclonal anti-VEGFR3 (Kubo et al., 2000), biotinylated polyclonal anti-mouse VEGFR3, anti-NRP2 and anti-VEGFC (R&D Systems, Oxon, UK), PECAM (Pharmingen, San Diego, CA) and FITC-conjugated anti-smooth muscle actin (Sigma). X-gal staining was carried out as described (Puri et al., 1995).

Lymphatic vessel counts

We prepared serial 7.5 μm transverse sections between the neck and the tail of E17 embryos (n=5 for $Nrp2^{-/-}$, n=4 for $Nrp2^{+/-}$, n=2 for $Nrp2^{+/+}$), which were ordered such that each slide contained sections from embryos of each genotype at the same anteroposterior level. These slides were stained with anti-VEGFR3 antibody (see Fig. 5C,E,G) and examined under the microscope (×25 objective, final magnification ×110). For body skin, the area counted spanned the dermis of the dorsal half of the embryo. In initial counts, different anteroposterior levels of the body axis were counted separately, i.e. between the forelimbs, around the waist and between the legs; no significant differences in these regions were observed and the data were pooled. For counts of hindlimb skin, the area considered was the dermis covering the entire hindlimb. We counted manually on every fourth section the number of VEGFR3-positive lymphatic profiles, a profile was counted as one regardless of its size (i.e. Fig. 5C $Nrp2^{+/-}$; 11 profiles counted). The length of the dermis was measured, its thickness was similar in all embryos analyzed (see Fig. 5C-H) and was therefore not taken into account. No significant differences in embryos of the same genotype were observed, and data for embryos of the same genotype were pooled. The count thus represents the mean±s.d. of the sum of all vessel profiles per cm of dorsal half of the dermis. For counts of subserosal VEFGFR3-positive lymphatic profiles, we proceeded in the same way.

BrdU incorporation

Pregnant females were injected intraperitoneally with 2 ml/100 g BrdU (Roche Diagnostics). After 6 hours, mice were sacrificed and embryos recovered for immunohistochemistry as described above. We used a biotinylated mouse anti-BrdU antibody (Pharmingen, San Diego, CA) and diaminobenzidine (Sigma). Slides were then incubated with biotinylated anti-VEGFR3 and developed after tyramide amplification with CY3.

Studies on lymphatic transport

FITC-dextran (2000 kDa, 8 mg/ml, Sigma) was injected intradermally into the ear and staining of the lymphatic network was followed by fluorescence stereomicroscopy.

RESULTS

NRP2 expression in the vascular system

We examined NRP2 expression during embryonic and postnatal stages (E10-P30) by in situ hybridization using a murine *Nrp2* antisense riboprobe (Chen et al., 1997). In addition, we performed immunostaining with an anti-NRP2

antibody and X-gal staining of heterozygous *Nrp2* mutant mice (Chen et al., 2000). These mice carry a gene trap insertion of a β-galactosidase reporter cassette fused to the CD4 transmembrane domain into an intron of the *Nrp2* locus, producing a non-functional fusion protein retained in the endoplasmic reticulum. During embryonic development, we observed essentially the same *Nrp2* mRNA expression pattern as previously described (Chen et al., 1997), including expression at E10 in the floor plate and neurons of the ventral region of the spinal cord, dorsal root and sympathetic ganglia, somitic tissue, and dorsal aspect of the forelimb (Fig. 1A). In addition, we observed expression of *Nrp2* in the vascular system. E10 mouse embryos showed a signal in EC of the cardinal vein, but not the dorsal aorta (Fig. 1A,D). The *Nrp1* receptor mRNA showed a complementary expression pattern in the dorsal aorta EC and in underlying mesenchymal cells, but was absent from the cardinal vein (Fig. 1B,E). Comparison with *Vegfr3* expression (Kaipainen et al., 1995) showed that mRNA for this receptor had already become downregulated in arterial and venous EC at E10, but remained high in small vessels that appeared to branch from the cardinal vein (Fig. 1C,F).

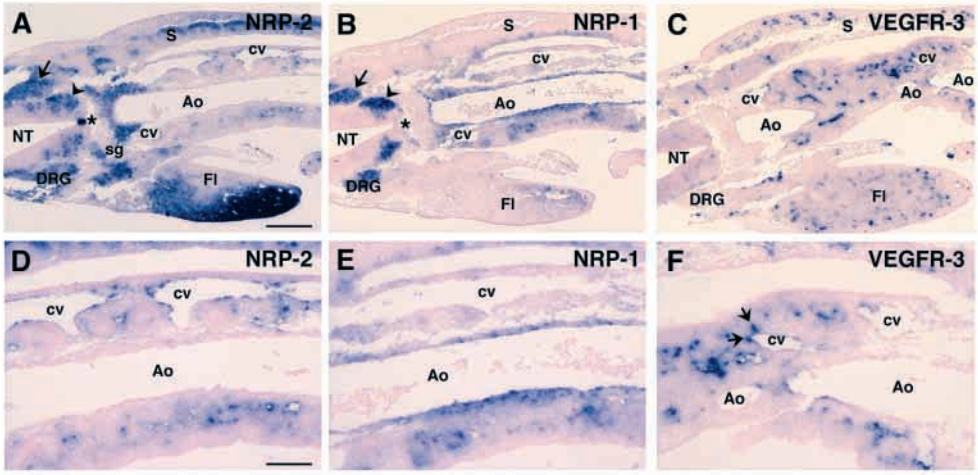

Fig. 1. NRP2 expression in the vascular system of E10 mouse embryos is restricted to veins. In situ hybridization with the indicated antisense riboprobes to sections of E10 mouse embryos. (A) *Nrp2* is expressed in the floor plate (asterisk), neurons of the ventral spinal cord (arrowhead), dorsal root ganglion (DRG, arrow), sympathetic ganglion (sg), somitic tissue (S) and dorsal aspect of the forelimb (Fl). (B) Overlapping, but distinct expression of *Nrp1*, which is expressed in neurons of the ventral spinal cord (arrowhead) and DRG (arrow). Asterisk indicates floor plate. (C) *Vegfr3* expression is restricted to the vascular system. (D-F) Higher magnification of the sections in A-C. *Nrp2* is expressed in the cardinal vein (cv, D), while *Nrp1* shows complementary expression in the aorta (Ao, E) and surrounding mesenchymal cells. (F) *Vegfr3* expression is low in EC of the aorta and cardinal vein, but high in small vessels that appear to branch from the cardinal vein (arrows in F). NT, neural tube. Scale bars: in A, 200 μm for A-C; in D, 95 μm for D-F.

During subsequent developmental stages, *Nrp2* mRNA and protein expression in the cardinal vein decreased to very low levels (Fig. 2A,D). From E13 onwards, the only vessels strongly expressing NRP2 appeared to be lymphatics, as judged initially by their anatomical position: in the neck region, the major lymphatic

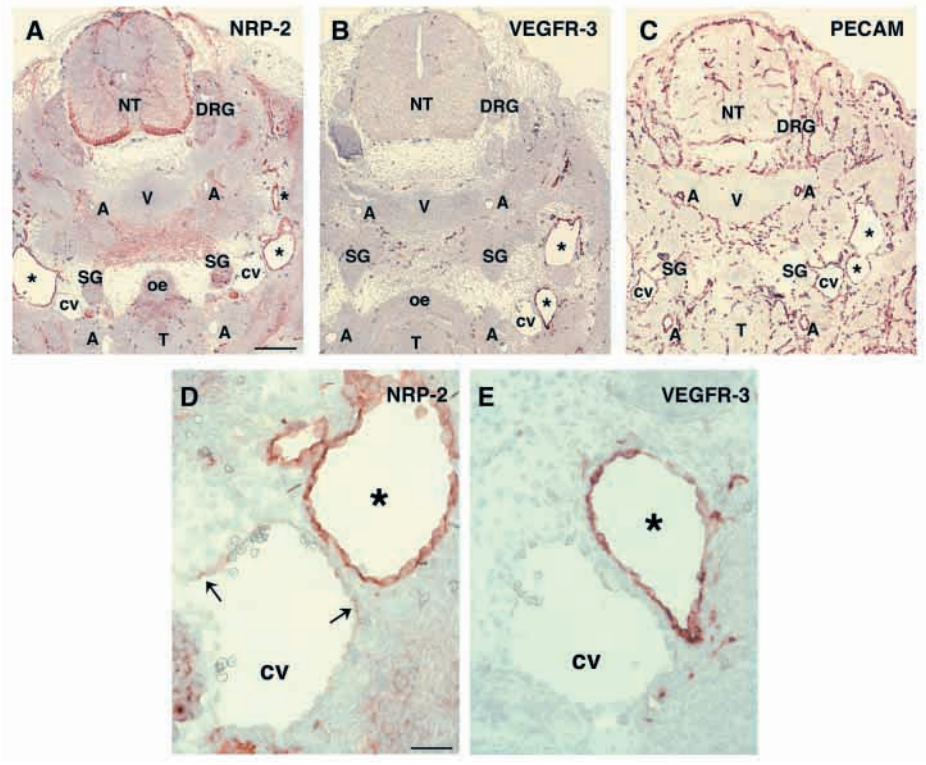

Fig. 2. *Nrp2* expression becomes restricted to embryonic lymphatic vessels and, at low levels, veins. Transverse adjacent sections through the neck of an E13 embryo stained with antibodies against the indicated proteins. (A) NRP2 is expressed in the ventral part of the neural tube (NT) and sympathetic ganglia (SG), as well as in mesenchyme surrounding the developing vertebrae (V) and trachea (T). In the vascular system, arteries (A) are negative, the cardinal veins (cv) are weakly positive and jugular lymphatic vessels (asterisks) are strongly positive. (B) VEGFR3 is expressed in the jugular lymphatic vessels (asterisks). (C) PECAM staining reveals abundant blood-vascular capillaries, arteries (A) and the cardinal veins (cv). Note expression on lymphatics at this developmental stage (asterisks). (D,E) High-power magnification of the cardinal vein (cv) and the adjacent lymphatic vessel (asterisk). Note weak NRP2 expression in the cv (arrows). DRG, dorsal root ganglion; oe, oesophagus. Scale bars: in A, 175 μm for A-C; in D, 35 μm for D,E.

vessels are formed in close proximity to the cardinal vein (Fig. 2). These vessels and their branches strongly expressed NRP2 (Fig. 2A,D). To precisely determine if the NRP2-positive vessels were lymphatics, we performed staining for VEGFR3, which is largely restricted to lymphatic EC (Kaipainen et al., 1995) and PECAM, which labels all EC but shows lower expression levels on mature lymphatic EC (Erhard et al., 1996). VEGFR3 and NRP2 both strongly labeled the jugular lymphatic vessels (Fig. 2A,B). Arteries did not express VEGFR3 or NRP2, but were strongly PECAM positive (Fig. 2A-C). Veins were PECAM positive, VEGFR3 negative and weakly labeled with NRP2 (Fig. 2C-E). This expression of NRP2 was maintained throughout development and persisted in the adult. Lymphatic EC of all tissues and organs examined (gut, mesenteries, skin, heart, lung, diaphragm) co-expressed NRP2 and the lymphatic EC markers VEGFR3 and podoplanin (Karkkainen and Alitalo, 2002) (Fig. 3). However, in all tissues and organs examined, NRP2 remained expressed at low levels in veins (Fig. 3A,D), which were not labeled with VEGFR3 or podoplanin antibodies (Fig. 3B,C,E-G). The expression of NRP2 therefore suggested possible functions in the development of veins and lymphatic vessels.

Analysis of vascular development in NRP2 mutant mice

To study the function of NRP2 in vascular development, we used *Nrp2* mutant mice previously described (Chen et al., 2000) (see Materials and Methods). The *Nrp2* mutation was bred into two genetic backgrounds, C57B6 and CD1, both were analyzed in this study and results were indistinguishable. Genotyping was performed using RT-PCR essentially as described (Chen et al., 2000). Homozygous *Nrp2* mutants were found to be viable, but were obtained at a reduced mendelian frequency. Of 328 mice analyzed between E13 and P30, the expected ratio of homozygous mutants was observed until P0 (175 animals: n=44 for $Nrp2^{-/-}$, n=86 for $Nrp2^{+/-}$, n=45 for $Nrp2^{+/+}$). Mice older than P1 were obtained at a reduced ratio (153 animals, n=29 for $Nrp2^{-/-}$, n=77 for $Nrp2^{+/-}$, n=47 for $Nrp2^{+/+}$). The reduced ratio of homozygotes was most probably due to the death of some animals between P0 and P1: 11/29 homozygous mice tested at P0 and P1 were dying. Death of these animals appeared unrelated to their vascular phenotype, which was similar in the dying and surviving mutants (see below). Additional causes for lethality may therefore exist, perhaps related to the neuronal phenotype of these mice (Chen et al., 2000; Giger et al., 2000). The surviving homozygous mutants could live until at least P30; however, they were smaller than their littermates (about 60% of body weight compared with $Nrp2^{+/-}$ or $Nrp2^{+/+}$ littermates). A difference in size was apparent from about P8 onwards. This phenotype had not been reported previously.

Different tissues of *Nrp2* mutants were examined on sections and by whole-mount X-gal staining. Serial transverse sections of E13 and E15 embryos (n=5 for $Nrp2^{-/-}$, n=10 for $Nrp2^{+/-}$, n=3 for $Nrp2^{+/+}$) were stained with PECAM antibodies, which revealed no differences in blood vessels and capillaries between $Nrp2^{-/-}$ and $Nrp2^{+/-}$ or $Nrp2^{+/+}$ animals (Fig. 4A-C). Staining with NRP2 and VEGFR-3 antibodies showed that jugular lymphatic vessels (Fig. 4D-I) as well as lymphatics of the thoracic duct were present and appeared normal. However, striking differences in the formation of lymphatic capillaries were noted between $Nrp2^{-/-}$ and $Nrp2^{+/-}$ or $Nrp2^{+/+}$ embryos from E13 until P3. In E13 $Nrp2^{+/+}$ and $Nrp2^{+/-}$ embryos, numerous VEGFR3- and NRP2-positive capillaries were present in the dermis (Fig. 4D,E,G,H). These capillaries were absent or strongly reduced in number in the $Nrp2^{-/-}$ littermates (Fig. 4F,I). NRP2 staining of sections of $Nrp2^{-/-}$ embryos confirmed their genotype: intracellular punctuate staining was observed instead of membrane staining, reflecting the retention of mutant protein in the endoplasmic reticulum (Fig. 4I).

To determine if the NRP2 mutation affected lymphatic capillary formation in the skin, we performed whole-mount X-gal staining of the skin of E15 embryos (n=8 for $Nrp2^{-/-}$, n=13 for $Nrp2^{+/-}$). An almost complete absence of X-gal-positive vessels was observed in the dorsal skin overlying the neural tube in $Nrp2^{-/-}$ animals, while the corresponding skin of $Nrp2^{+/-}$ mice showed a readily visible capillary plexus (Fig. 5A,B). We next prepared serial transverse sections between the neck and the tail of E17 embryos (n=8 for $Nrp2^{-/-}$, n=8 for $Nrp2^{+/-}$, n=5 for $Nrp2^{+/+}$), which were ordered such that each slide contained sections from $Nrp2^{+/+}$,

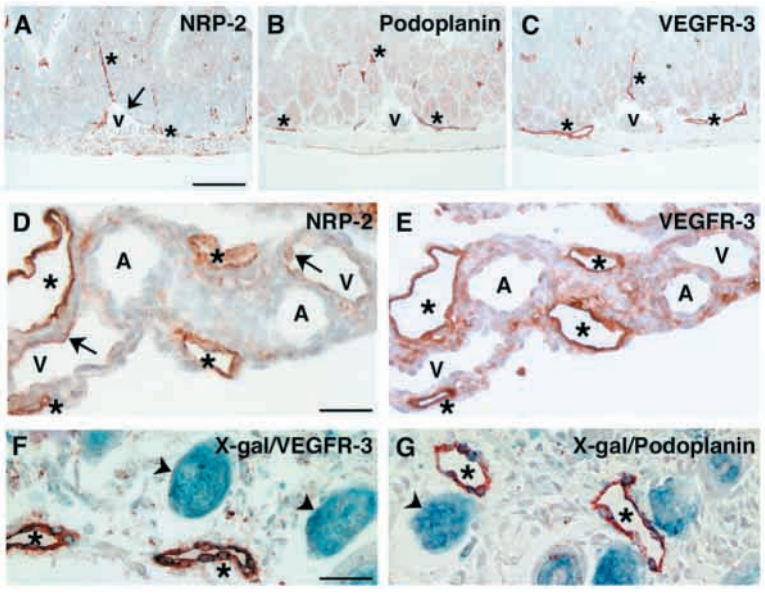

Fig. 3. *Nrp2* expression in adult vessels. (A-C) Transverse sections of P30 gut from a $Nrp2^{+/-}$ mouse stained with antibodies directed against the indicated proteins. Note co-expression of NRP2 (A) with the lymphatic markers podoplanin (B) and VEGFR3 (C) in subserosal lymphatic vessels (asterisks). Weak NRP2 expression is observed in a subserosal vein (v, arrow). NRP2 is also expressed in the smooth-muscle layer surrounding the gut (Chen et al., 1997), punctuate staining reflects loss of one wild-type allele. (D,E) Staining of $Nrp2^{+/+}$ P0 mesentery sections with the indicated antibodies. Note co-expression of NRP2 and VEGFR3 in lymphatics (asterisks), weaker expression of NRP2 in veins (V, arrows), and absence of expression in arteries (A). (F,G) P0 skin section from a $Nrp2^{+/-}$ mouse double-stained with X-gal (blue staining) and VEGFR3 (F) or podoplanin (G) antibodies (brown staining). Note double-stained lymphatics (asterisks). NRP2 also labels hair-follicles (arrowheads). Scale bars: in A, 140 μm for A-C; in D, 35 μm for D,E; in F, 40 μm for F,G.

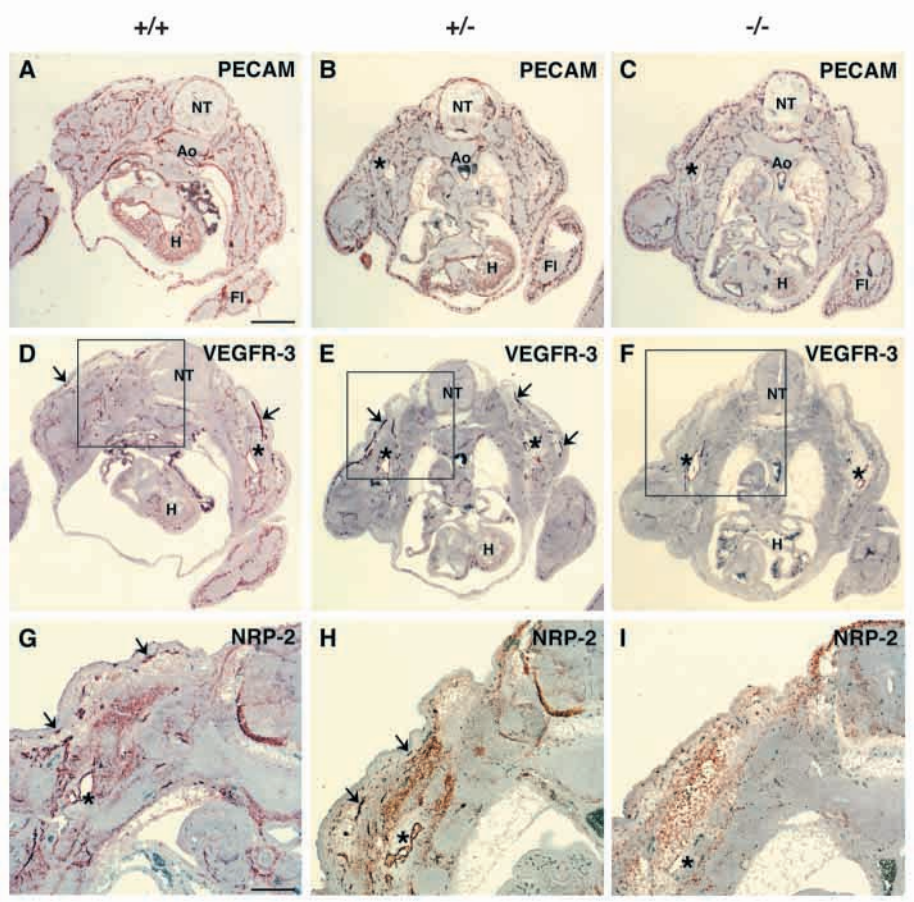

Fig. 4. Lymphatic vessel defects in E13 *Nrp2* mutant embryos. Transverse sections of E13 $Nrp2^{+/+}$ (A,D,G), $Nrp2^{+/-}$ (B,E,H) and $Nrp2^{-/-}$ (C,F,I) embryos stained with antibodies recognizing the indicated proteins. Note very similar PECAM staining in the three genotypes (A-C). (D-F) VEGFR3 labels jugular lymphatic vessels (asterisks) present in all three genotypes, as well as lymphatic capillaries in the skin (arrows). Note absence of these capillaries in the $Nrp2^{-/-}$ embryo (F). (G-I) Higher magnification of adjacent sections corresponding to the boxed area in D-F stained with NRP2 antibodies. The jugular lymphatic vessel (asterisk) is present in all three genotypes. Skin capillaries are NRP2 positive in the $Nrp2^{+/+}$ (G) and the $Nrp2^{+/-}$ (H) embryo. In the $Nrp2^{-/-}$ embryo (I), only punctuate staining is observed, reflecting the retention of mutant protein in the endoplasmic reticulum. Ao, aorta; Fl, forelimb; H, heart; NT, neural tube. Scale bars: in A, 575 μm for A-F; in G, 230 μm for G-I.

$Nrp2^{+/-}$ and $Nrp2^{-/-}$ embryos. Sections of the skin of newborn mice were also prepared (n=12 for $Nrp2^{-/-}$, n=16 for $Nrp2^{+/}$, n=7 for $Nrp2^{+/+}$). These slides were stained with antibodies recognizing VEGFR3, PECAM and smooth-muscle actin (SMA). In all cases except one (P0), a reduction of the number of VEGFR3-positive vessels was observed in $Nrp2^{-/-}$ mutants as compared to $Nrp2^{+/-}$ or $Nrp2^{+/+}$ skins (Fig. 5C,E,G). By contrast, PECAM staining did not reveal a reduction in the number of dermal blood-vascular capillaries, arteries or veins (Fig. 5D,F,H). In all mice analyzed, PECAM staining of the VEGFR3-positive lymphatic vessels in the skin was less intense than staining of arteries or veins (Fig. 5E,F). In contrast to arteries and veins, VEGFR3-positive lymphatic vessels were not surrounded by SMA-positive cells (Fig. 5I,J). The VEGFR3-positive lymphatic vessels that formed in the $Nrp2^{-/-}$ mice sometimes appeared enlarged and were present at the border of the dermis and the subcutaneous tissue, when compared with $Nrp2^{+/+}$ and $Nrp2^{+/-}$ littermates, where most of them were present roughly in the middle layer of the dermis (Fig. 5C,E,G).

The number of VEGFR3-positive lymphatic vessels present in the skin was counted on transverse serial sections of E17 embryos (n=5 for $Nrp2^{-/-}$, n=4 for $Nrp2^{+/-}$, n=2 for $Nrp2^{+/+}$) (see Materials and Methods). No significant difference in lymphatic vessel number was observed in $Nrp2^{+/+}$ compared with $Nrp2^{+/-}$ skins (vessel number per cm sectioned body skin 20.6±1.1 in $Nrp2^{+/+}$, 19.4±1.1 in $Nrp2^{+/-}$; hindlimb skin 31.7±5.3 in $Nrp2^{+/+}$, 32.4±2.0 in $Nrp2^{+/-}$). In $Nrp2^{-/-}$ embryos, the lymphatic vessel number was reduced three times in the body skin (vessel number per cm=6.1±1.7) and 1.8 times in the skin of the limb (18.0±2.3). To monitor the proliferation of lymphatic EC, we measured BrdU incorporation into the lymphatic vessels of the body skin of E17 embryos (n=5 for $Nrp2^{-/-}$, n=3 for $Nrp2^{+/-}$, n=1 for $Nrp2^{+/+}$). In the $Nrp2^{+/+}$ and $Nrp2^{+/-}$ mice, 23.9±3.7% of VEGFR3-positive cells had incorporated BrdU (Fig. 6A,C), while only 13.6±3.4% of VEGFR3-positive cells were also BrdU positive in the $Nrp2^{-/-}$ mutants (Fig. 6B,D). Thus, a reduction of about 1.8-fold was observed in the proliferation of skin lymphatic vessels in E17 *Nrp2* mutants. By contrast, no obvious decrease in the number of BrdU-positive cells in the epidermis (Fig. 6A,B) or other tissues was detected in the $Nrp2^{-/-}$ animals compared with $Nrp2^{+/-}$ or $Nrp2^{+/+}$.

Whole-mount X-gal staining also revealed the absence or strong reduction of the number of lymphatic capillaries at the surface of the heart in the $Nrp2^{-/-}$ compared with $Nrp2^{+/-}$ littermates (Fig. 7A,B). Staining of sections prepared from hearts with VEGFR3 antibody confirmed that the X-gal stained vessels were lymphatics (Fig. 7C). The onset of the phenotype correlated with the onset of the development of these vessels: X-gal-positive lymphatic capillaries progressively covered the heart surface from E15 onwards in $Nrp2^{+/-}$ mutants, while in $Nrp2^{-/-}$ embryos, only collecting lymphatic trunks surrounding the great vessels were present at all developmental stages examined (Fig. 7A,B).

In the periphery of the diaphragm, a striking reduction of the

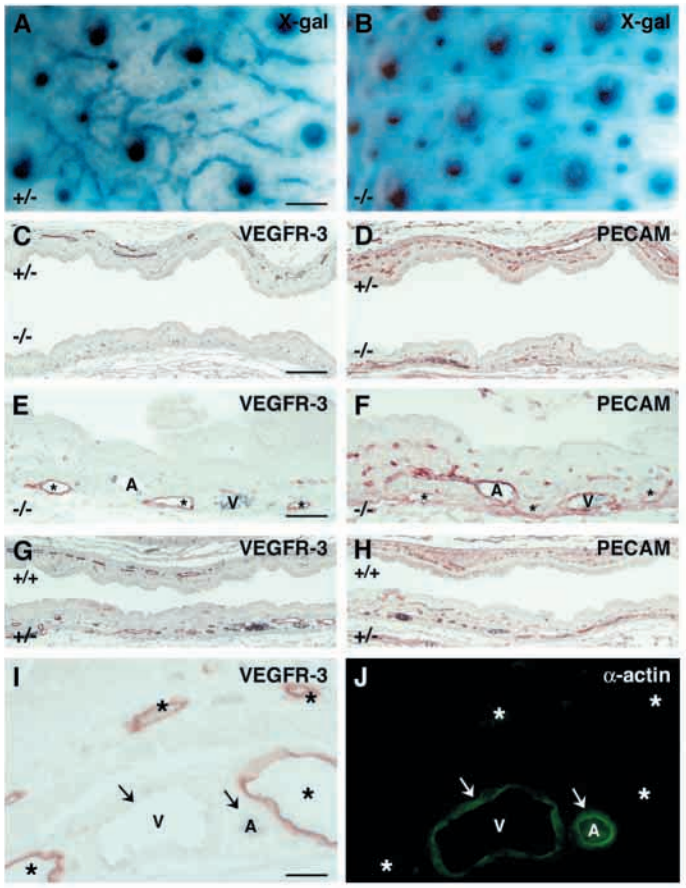

Fig. 5. Lymphatic vessel defects in the skin of developing *Nrp2* mutant mice. (A,B) Whole-mount X-gal staining of E15 dorsal skin. Note the absence of X-gal-positive vessels in the $Nrp2^{-/-}$ (B). (C-H) Transverse sections through the dorsal skin of E17 embryos stained with anti-VEGFR3 (C,E,G) and PECAM (D,F,H). Note the absence of lymphatic vessels in the $Nrp2^{-/-}$ dermis (C, bottom) compared with $Nrp2^{+/+}$ and $Nrp2^{+/-}$ dermis (C, top; G). PECAM staining shows no difference between the three genotypes (D,H). (E,F) Comparison of VEGFR3 and PECAM staining of a $Nrp2^{-/-}$ dermis at higher magnification. Note weaker PECAM staining of VEGFR3-positive vessels (asterisks) as compared with arteries (A) and veins (V). Note also that the lymphatic vessels that form are located in a slightly deeper position at the border of the dermis and the connective tissue (compare E with C, G). (I,J) The comparison of VEGFR3 and α-actin staining shows that lymphatic vessels (asterisks) are not surrounded by smooth-muscle cells, while arteries and veins are (A, V, arrows). Scale bars: in A, 230 μm for A,B; in C, 180 μm for C,D,G,H; in E, 70 μm for E,F; in I, 20 μm for I,J.

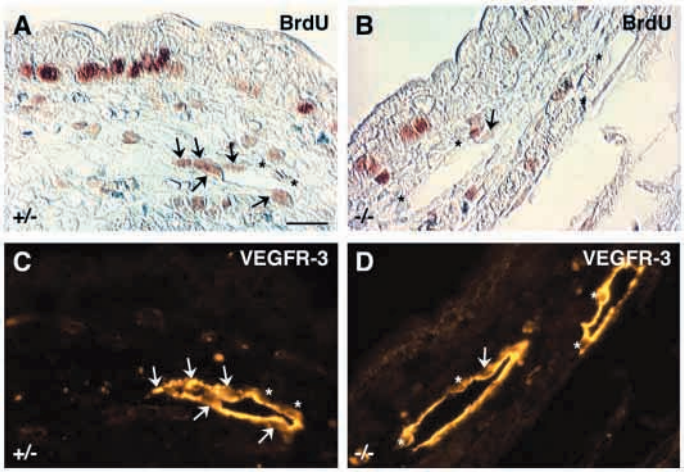

Fig. 6. BrdU incorporation in lymphatic vessels is decreased in mutant skins. (A,B) Bright-field images showing BrdU-positive (arrows) and -negative (asterisks) nuclei in lymphatic EC from sectioned E17 embryos. (C,D) Lymphatic EC were identified by double-staining with VEGFR3 antibody. Note the decreased number of BrdU-positive nuclei in the $Nrp2^{-/-}$ (arrows in B,D) Scale bar: 30 μm.

number of X-gal-positive capillaries was observed from E15 onwards (Fig. 7F,G). Sectioning of X-gal-stained diaphragms and labeling with VEGFR3 antibodies confirmed that these capillaries were lymphatics (Fig. 7H,I). The onset of this phenotype coincided with the onset of the development of these capillaries between E15 and E17. Larger collecting lymphatics in the central portion of the diaphragm were present in the $Nrp2^{-/-}$ animals and appeared normal (Fig. 7F,G). Some weaker X-gal-stained vessels, which may correspond to veins or to larger collecting lymphatic vessels, were present in all $Nrp2^{-/-}$ mutants (Fig. 7G).

Altogether, of 36 $Nrp2^{-/-}$ hearts and diaphragms examined between E15 and P3, 32 hearts showed an absence of lymphatic capillaries, the remaining four resembled $Nrp2^{+/-}$ mice. All diaphragms showed absence of lymphatic vessels; so all the 36 $Nrp2^{-/-}$ mice could be clearly distinguished from their $Nrp2^{+/-}$ littermates by X-gal staining of these two tissues. Hearts and diaphragms of $Nrp2^{+/-}$ mice (n=106) always showed a similar staining pattern (Fig. 7A,F). Staining with an antibody recognizing VEGF-C revealed labeling of the superficial epicardium in both $Nrp2^{-/-}$ and $Nrp2^{+/-}$ mice (Fig. 7D,E), suggesting that the observed decrease in lymphatic vessel density was not due to decreased levels of this growth factor.

To analyze a possible phenotype in the lung, we performed X-gal staining, VEGFR3 whole-mount immunohistochemistry of lung slices (not shown) and staining of transverse lung sections (n=3 for $Nrp2^{-/-}$, n=3 for $Nrp2^{+/-}$ sectioned at E15; n=1 for $Nrp2^{-/-}$, n=1 for $Nrp2^{+/-}$, n=1 for $Nrp2^{+/+}$ at E17; n=4 for $Nrp2^{-/-}$, n=4 for $Nrp2^{+/-}$, n=2 for $Nrp2^{+/+}$ at P0) with antibodies directed against NRP2, VEGFR-3 and PECAM. Lymphatics of the thoracic duct were present in the $Nrp2^{-/-}$ mice at all stages examined (Fig. 8A,B). However, lymphatic capillaries, numerous in $Nrp2^{+/-}$ or $Nrp2^{+/+}$ lungs, were strongly reduced in $Nrp2^{-/-}$ lungs (Fig. 8A,B,E-G). This phenotype was observed from E15 onwards and correlated with the appearance of VEFGR3-positive capillaries in the lungs at E15. PECAM staining did not reveal any differences in the blood-vascular EC of the different animals (Fig. 8C,D). At birth, lymphatic vessels surrounding the main bronchi had formed in the $Nrp2^{-/-}$ lungs and were stained with anti-NRP2 and VEGFR3 antibodies (Fig. 8E-G). However, VEGFR3-positive capillaries were still absent in the $Nrp2^{-/-}$ mutants (Fig. 8E-G). In the subserosal plexus of the gut, a reduction in the number of lymphatic vessels was observed in E15 and E17 embryos (Fig. 8H,I). Counting of the number of VEGFR3-positive vessels in the subserosal plexus confirmed this reduction: 5.2±0.4 VEGFR3-positive vessels per cm sectioned

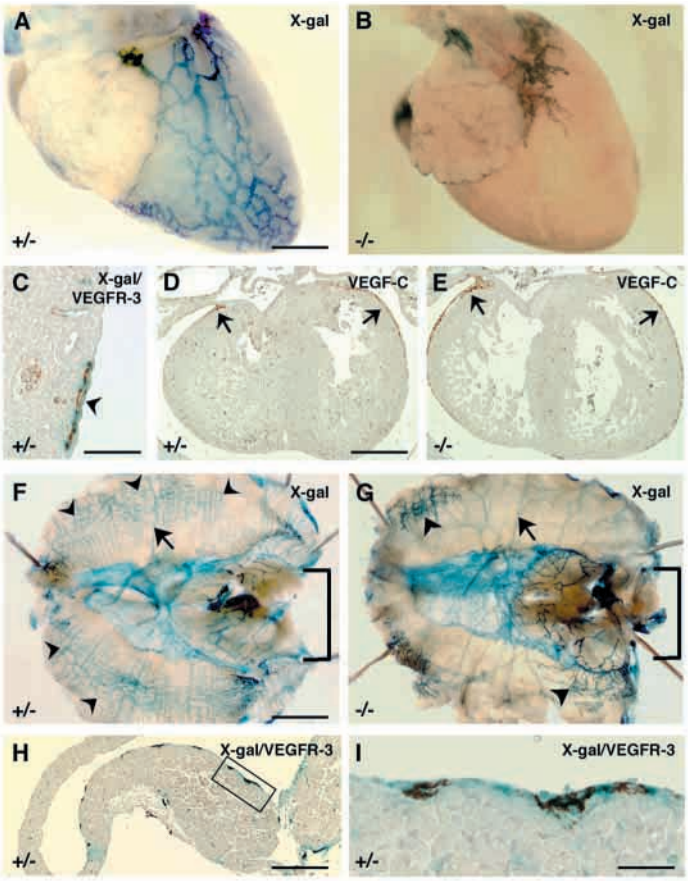

Fig. 7. Lymphatic vessel defects in the heart and diaphragm of *Nrp2* mutants. (A,B) Whole-mount X-gal staining of P0 hearts showing the reduction of capillaries in the $Nrp2^{-/-}$ heart (B). (C) Double-staining of the X-gal-positive vessels present at the epicardial surface of $Nrp2^{+/-}$ embryos (arrowhead) with anti-VEGFR3 (brown staining). (D,E) Transverse sections of E15 hearts stained with anti-VEGF-C antibodies. Note staining of the superficial epicardium in both $Nrp2^{+/-}$ and $Nrp2^{-/-}$ (D,E, arrows). (F,G) Whole-mount X-gal staining of P0 diaphragms (thoracic view). Note the reduction of peripheral X-gal-positive lymphatic capillaries (arrowheads) in the $Nrp2^{-/-}$ diaphragm. Brackets outline the central portion of the diaphragm, which is unaffected. Weaker NRP2 expression in veins is also indicated (arrows). H. Double-staining of the X-gal-positive vessels present in the diaphragm of $Nrp2^{+/-}$ embryos with anti-VEGFR3 (brown staining) confirms that they are lymphatics. (I) Higher magnification of the boxed region in H. Scale bars: in A, 580 μm for A,B; in C, 50 μm; in D, 360 μm for D,E; in F, 1400 μm for F,G; in H, 270 μm; in I, 40 μm.

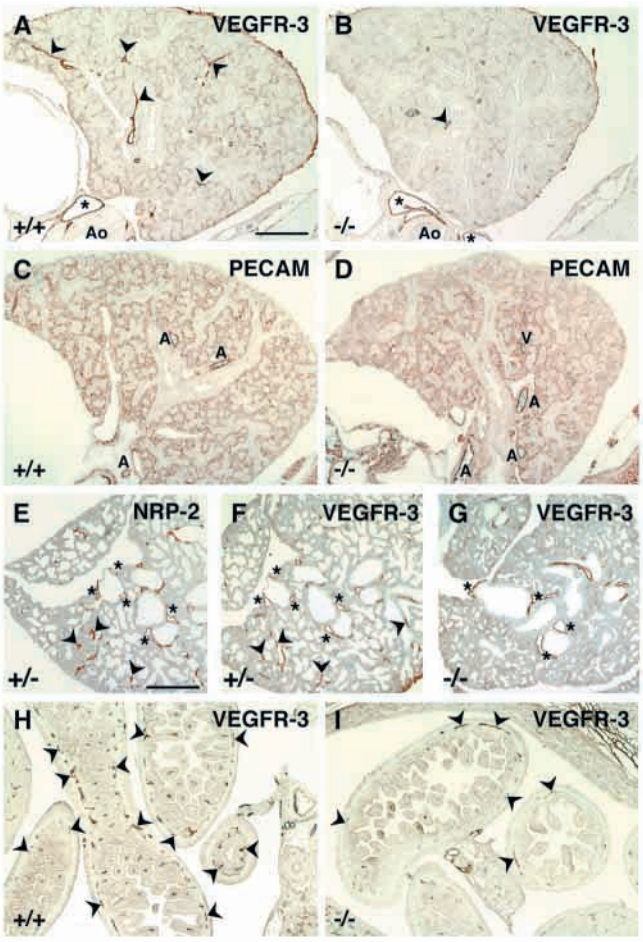

Fig. 8. Lymphatic vessel defects in the lung and the gut of *Nrp2* mutants. (A-G) Transverse sections of the lung of E17 (A-D) and P0 (E-G) mice stained with antibodies directed against the indicated proteins. (A,B) Note presence of lymphatics of the thoracic duct in both $Nrp2^{+/+}$ and $Nrp2^{-/-}$ embryos (asterisks), while VEGFR3-positive capillaries in the $Nrp2^{-/-}$ lung are almost completely absent (arrowheads, A,B). (C,D) PECAM staining of the alveolar blood-vascular capillaries is uniform in both genotypes, arteries (A) and veins (V) are also present in both genotypes. (E,F) Co-expression of VEGFR3 and NRP2 in larger lymphatics (asterisks), as well as in numerous capillaries (E,F, arrowheads). (G) Lymphatic capillaries are absent in $Nrp2^{-/-}$ lung, while lymphatics surrounding the bronchi are present (asterisks). (H,I) Transverse sections through the gut of E17 embryos. Note numerous subserosal VEGFR3-positive vessels in the $Nrp2^{+/+}$ gut, which are reduced in the $Nrp2^{-/-}$ gut (H, I, arrowheads). Scale bars: in A, 275 μm for A-D,H,I; in E, 325 μm for E-G. Ao, aorta.

guts were observed in $Nrp2^{+/-}$ and $Nrp2^{+/+}$ animals (n=4 sectioned at E17), while 2.3±0.7 vessels were counted per cm sectioned guts in $Nrp2^{-/-}$ littermates (n=5).

Lymphatic vessels can form in mutant animals

Lack of lymphatic skin vessels is associated with hereditary or acquired lymphoedema (Karkkainen et al., 2000; Karkkainen et al., 2001). No signs of dermal thickening or oedema in the extremities of newborn, juvenile or adult *Nrp2* mutant mice were, however, apparent. To determine the evolution of the lymphatic vessels in the skin of older *Nrp2* mutants, we carried out a functional test based on the uptake of high molecular weight FITC-dextran into the lymphatics after intradermal injection into the ear or the tail of P7 (n=1 for $Nrp2^{-/-}$, n=1 for $Nrp2^{+/+}$) and 4-week-old mice (n=5 for $Nrp2^{-/-}$, n=4 for $Nrp2^{+/-}$, n=3 for $Nrp2^{+/+}$). No difference in dye uptake between different animals could be observed (Fig. 9A,B). Sectioning of ears showed the presence of VEGFR3 and NRP2 stained lymphatic vessels (not shown). Thus, growth of lymphatic vessels and capillaries occurred during postnatal life in the mutant mice.

X-gal or VEGFR-3 staining of other organs isolated from juvenile or adult animals confirmed this observation. We analyzed hearts and diaphragms from seven $Nrp2^{-/-}$, three $Nrp2^{+/-}$ and four $Nrp2^{+/+}$ animals sacrificed between P7 and P12, as well as six $Nrp2^{-/-}$, five $Nrp2^{+/-}$ and four $Nrp2^{+/+}$ animals sacrificed between P20 and P35. In the heart, four out of seven $Nrp2^{-/-}$ mice between P7 and P12 showed very few lymphatic vessels, the remaining three resembled $Nrp2^{+/-}$. Older $Nrp2^{-/-}$ mutants always showed lymphatic vessels, although mostly with an abnormal pattern (Fig. 9C,D). In the diaphragm, all juvenile and adult $Nrp2^{-/-}$ mice showed lymphatic vessel growth (not shown). In the gut, the subserosal lymphatic plexus had formed in the $Nrp2^{-/-}$ mice at P0, as judged by whole-mount immunohistochemistry with VEGFR3 antibody (not shown). Transport of lipids into the mesenteries occurred normally in the $Nrp2^{-/-}$ mutants from birth onwards, as judged by visual inspection of milk uptake into the mesenteries after feeding (Fig. 9E,F). However, subserosal lymphatic vessels of adult mice were often enlarged (Fig. 9G,H). Lymph nodes were present in all mutant animals (not shown).

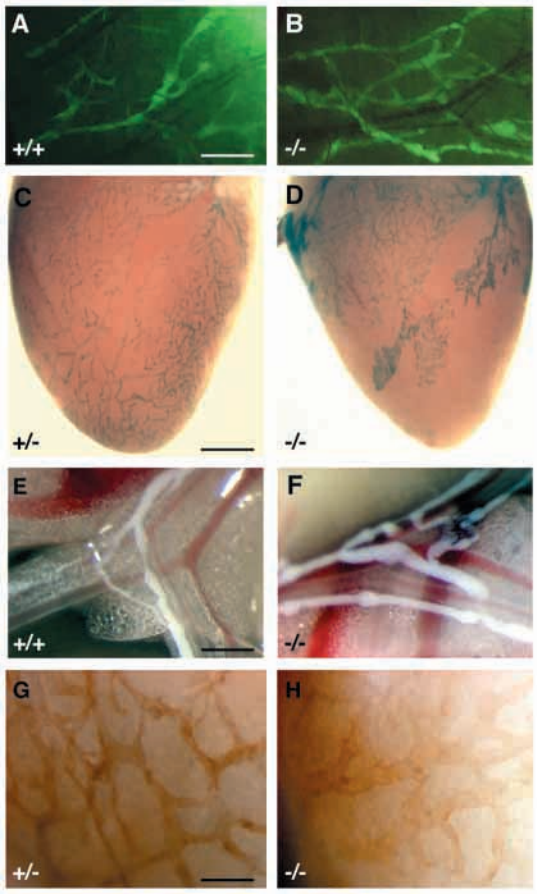

Fig. 9. Lymphatic vessels of adult *Nrp2* mutant mice. (A,B) FITC-dextran injection into ears of P30 mice. (C,D) Whole-mount X-gal staining of P30 hearts. Note the abnormal lymphatic vessels in the $Nrp2^{-/-}$ heart. (E,F) Milk-uptake after feeding in the mesenteries of $Nrp2^{+/+}$ and $Nrp2^{-/-}$ mice. (G,H) Whole-mount VEGFR3 immunostaining of P30 guts. Note enlarged lymphatic vessels in the $Nrp2^{-/-}$ gut. Scale bars: in A, 430 μm for A,B; in C, 1010 μm for C,D; in E, 390 μm for E,F; in G, 575 μm for G,H.

DISCUSSION

The data presented show a selective requirement for NRP2 in the formation of lymphatic vessels. Loss of NRP2 function resulted in the absence or severe reduction of the number of small lymphatic vessels and capillaries in all tissues examined, including the skin, gut, heart, diaphragm and lung. Lymphatic vessel number in all of these tissues was decreased as soon as these vessels developed in the embryo, and remained reduced or absent until after birth. BrdU incorporation studies revealed a reduction in the number of proliferating lymphatic EC in the skin, suggesting a requirement of NRP2 in the proliferation of these vessels. The lymphatic vessels present in the skin of mutant animals were also positioned abnormally and sometimes enlarged, suggesting that guidance defects may also occur in the absence of NRP2 function. Veins, which express lower levels of NRP2, developed normally in the $Nrp2^{-/-}$ animals and PECAM staining revealed no difference in capillary formation between homo- and heterozygous mice, suggesting that the NRP2 mutation selectively affected the lymphatic compartment.

The mechanisms responsible for the development of lymphatic vessels are currently not well understood. The first detectable lymphatic vessels in the embryo are the thoracic duct and jugular lymph sacs, which are thought to develop by sprouting from veins (Sabin et al., 1909). Indeed, labeling with lymphatic-specific markers such as Prox1 (Wigle and Oliver, 1999) or VEGFR3 (Kaipainen et al., 1995) are suggestive of a sprouting process. NRP2 is likely to be downstream of these initial events in the formation of lymphatic EC, as its expression becomes downregulated in veins after that of VEGFR3. Wigle et al. (Wigle et al., 2002) have recently shown that in Prox1 mutant mice, the initial sprout formation from veins is not affected, but that sprout progression is impaired and that the lymphatic EC instead adopt a blood-vascular phenotype. How the remaining lymphatic vessels in the body develop is currently unknown. Quail-chick chimera experiments have suggested the participation of mesoderm-derived lymphangioblasts (Wilting et al., 2000), but the extent of their contribution to the developing lymphatic vasculature is currently unknown. Our observations of NRP2 staining suggest that there is a phase of lymphatic EC development from pre-existing lymphatic EC, analogous to the classically defined angiogenesis process. NRP2 staining carried out at different stages of development showed a progressive coverage of, for example, the heart and the diaphragm with lymphatic EC. These vessels did not appear to develop by sprouting from veins; they may be formed by mesoderm-derived lymphangioblasts, but the most likely explanation is that they are formed by sprouting from pre-existing lymphatic vessels. In homozygous NRP2 mutants, this sprouting process appears affected, while the formation of the lymphatic thoracic duct and other collecting lymphatic vessels occurs normally. It may therefore be speculated that NRP2 function is not required for sprouting of lymphatic vessels from veins, but for the sprouting of lymphatic EC from pre-existing lymphatic EC. The *Nrp2* mutants analyzed here were previously reported to maintain very low levels of wild-type transcripts (Chen et al., 2000). Their neural phenotype was indistinguishable from a complete loss-of-function mutant generated by Giger et al. (Giger et al., 2000). The vascular

phenotype of this second *Nrp2* mutant has not been reported yet.

In the developing avian vascular system, expression of *Nrp1* and *Nrp2* has recently been shown to localize to arteries and veins, respectively (Moyon et al., 2001; Herzog et al., 2001). Preferential expression of NRP1 in developing retinal arteries has also been recently reported in mice (Stalmans et al., 2002). The observations reported here confirm and extend these findings: at early developmental stages, *Nrp1* and *Nrp2* are expressed in respectively arterial and venous EC. At later developmental stages, NRP2 mRNA and protein expression in veins decreases, but remains high in lymphatic EC, which can be also identified by expression of VEGFR3. The different expression patterns suggest non-redundant functions of NRP1 and NRP2 in the vascular system. Interestingly, inactivation of both *Nrp1* and *Nrp2* genes leads to embryonic lethality at E8.5 (Takashima et al., 2002). Embryos homozygous for one NRP mutation and heterozygous for the other NRP gene died at E10-E10.5 because of deficiencies in arterial and venous branching (Takashima et al., 2002). Taken together with the specific expression of *Nrp1* and *Nrp2* in respectively arterial and venous EC, these results suggest a requirement of both NRP genes for correct arterial and venous patterning during early remodeling of the primary vascular plexus. At later developmental stages, the *Nrp1* mutation mainly affects the arterial compartment (Kawasaki et al., 1999), while we here report a specific requirement for NRP2 in lymphatic EC.

NRP2 is co-expressed with VEGFR-3 in lymphatic EC, although in mature vessels of adult skin its levels were decreased, and it has been shown to bind VEGFC (Karkkainen et al., 2001). It is therefore tempting to speculate that NRP2 may act as a co-receptor for VEGFR3 to mediate VEGFC-dependent lymphangiogenesis, analogous to NRP1, which enhances VEGF165 activity via VEGFR2. However, biochemical analysis of the signal transduction initiated by NRP2 has yet to be performed. Mutations in the tyrosine kinase domain of VEGFR3 lead to cutaneous aplasia of lymphatic vessels, causing the formation of edema in both mouse and humans (Karkkainen et al., 2000; Karkkainen et al., 2001). No signs of edema were apparent in NRP2 mutant mice, in spite of the reduction of lymphatic vessels in the skin and the internal organs. Larger collecting lymphatic vessels were, however, present in the mutant animals, which may be sufficient for tissue fluid drainage. Furthermore, from P7 onwards we observed growth of lymphatic vessels in the different organs of $Nrp2^{-/-}$ animals. Regrowth of lymphatic vessels during postnatal development has also been observed in transgenic mice overexpressing a soluble VEGFR3 (Makinen et al., 2001). The precise mechanisms regulating embryonic and adult physiological and pathological lymphangiogenesis remain to be fully explored.

We thank M. Tessier-Lavigne for mice, A. Chédotal for probes, S. Gallier for animal care, P. Pourcelot for help with histology, members of the InsermU36 for discussion, and M. Tessier-Lavigne, A. Chédotal, J. L. Thomas, P. Corvol and J. Favier for reading the manuscript. This work was supported by grants from Association pour la Recherche contre le Cancer (ARC), Fondation pour la Recherche Médicale, Ministère de la Recherche (ACI) and Inserm (Avenir) to A. E. D. M. is supported by an ARC fellowship.

REFERENCES

Carmeliet, P., Ferreira, V., Breier, G., Pollefeyt, S., Kieckens, L., Gertsenstein, M., Fahrig, M., Vandenhoeck, A., Harpal, K., Eberhardt, C. et al. (1996). Abnormal blood vessel development and lethality in embryos lacking a single VEGF allele. *Nature* **380**, 435-439.

Chen, H., Chedotal, A., He, Z., Goodman, C. S. and Tessier-Lavigne, M. (1997). Neuropilin-2, a novel member of the neuropilin family, is a high affinity receptor for the semaphorins Sema E and Sema IV but not Sema III. *Neuron* **19**, 547-559.

Chen, H., Bagri, A., Zupicich, J. A., Zou, Y., Stoeckli, E., Pleasure, S. J., Lowenstein, D. H., Skarnes, W. C., Chedotal, A. and Tessier-Lavigne, M. (2000). Neuropilin-2 regulates the development of selective cranial and sensory nerves and hippocampal mossy fiber projections. *Neuron* **25**, 43-56.

Detmar, M., Brown, L. F., Schon, M. P., Elicker, B. M., Velasco, P., Richard, L., Fukumura, D., Monsky, W., Claffey, K. P. and Jain, R. K. (1998). Increased microvascular density and enhanced leukocyte rolling and adhesion in the skin of VEGF transgenic mice. *J. Invest. Dermatol.* **111**, 1-6.

Erhard, H., Rietveld, F. J., Brocker, E. B., de Waal, R. M. and Ruiter, D. J. (1996). Phenotype of normal cutaneous microvasculature. Immunoelectron microscopic observations with emphasis on the differences between blood vessels and lymphatics. *J. Invest. Dermatol*. **106**, 135-140.

Feiner, L., Koppel, A. M., Kobayashi, H. and Raper, J. A. (1997). Secreted chick semaphorins bind recombinant neuropilin with similar affinities but bind different subsets of neurons in situ. *Neuron* **19**, 539-545.

Ferrara, N., Carver-Moore, K., Chen, H., Dowd, M., Lu, L., O'Shea, K. S., Powell-Braxton, L., Hillan, K. J. and Moore, M. W. (1996). Heterozygous embryonic lethality induced by targeted inactivation of the VEGF gene. *Nature* **380**, 439-442.

Giger, R. J., Cloutier, J. F., Sahay, A., Prinjha, R. K., Levengood, D., Moore, S. E., Pickering, S., Simmons, D., Rastan, S., Walsh, F. S. et al. (2000). Neuropilin-2 is required in vivo for selective axon guidance responses to secreted smeaphorins. *Neuron* **25**, 29-41.

He, Z. and Tessier-Lavigne, M. (1997). Neuropilin is a receptor for the axonal chemorepellent semaphorin III. *Cell* **90**, 739-751.

Herzog, Y., Kalcheim, C., Kahane, N., Reshef, R. and Neufeld, G. (2001). Differential expression of neuropilin-1 and neuropilin-2 in arteries and veins. *Mech. Dev.* **109**, 115-119.

Jeltsch, M., Kaipainen, A., Joukov, V., Meng, X., Lakso, M., Rauvala, H., Swartz, M., Fukumura, D., Jain, R. K. and Alitalo, K. (1997). Hyperplasia of lymphatic vessels in VEGF-C transgenic mice. *Science* **276**, 1423-1425.

Kaipainen, A., Korhoonen, J., Mustonen, T., van Hinsbergh, V., Fong, G. H., Dumont, D., Breitman, M. L. and Alitalo, K. (1995). Expression of the fms-like tyrosine kinase 4 gene becomes restricted to lymphatic endothelium during development. *Proc. Natl. Acad. Sci. USA* **92**, 3566-3570.

Karkkainen, M. J., Ferrell, R. E., Lawrence, E. C., Kimak, M. A., Levinson, K. L., McTigue, M. A., Alitalo, K. and Finegold, D. N. (2000). Missense mutations interfere with VEGFR-3 signaling in primary lymphoedema. *Nat. Genet.* **25**, 153-159.

Karkkainen, M. J., Saaristo, A., Jussila, L., Karila, K. A., Lawrence, E. C., Pajusola, K., Bueler, H., Eichmann, A., Kettunen, M. I., Ylä-Herttuala, S. et al. (2001). A model for gene therapy of human reditary lyphedema. *Proc. Natl. Acad. Sci. USA* **98**, 12677-12682.

Karkkainen, M. J. and Alitalo, K. (2002). Lymphatic endothelial regulation, lymphoedema, and lymph node metastasis. *Semin. Cell Dev. Biol*. **13**, 9-18.

Karkkainen, M. J., Mäkinen, T. and Alitalo, K. (2002). Lymphatic endothelium: a new frontier of metastasis research. *Nat. Cell Biol.* **4**, E2-E5.

Karpanen, T., Egeblad, M., Karkkainen, M. J., Kubo, H., Yla-Herttuala, S., Jaattela, M. and Alitalo, K. (2001). Vascular endothelial growth factor C promotes tumor lymphangiogensis and intralymphatic tumor growth. *Cancer Res.* **61**, 1786-1790.

Kawasaki, T., Kitsukawa, T., Bekku, Y., Matsuda, Y., Sanbo, M., Yagi, T. and Fujisawa, H. (1999). A requirement for neuropilin-1 in embryonic vessel formation. *Development* **126**, 4895-4902.

Kitsukawa, T., Shimizu, M., Sanbo, M., Hirata, T., Taniguchi, M., Bekku, Y., Yagi, T. and Fujisawa, H. (1997). Neuropilin-semaphorin III/D-mediated chemorepulsive signals play a crucial role in peripheral nerve projection in mice. *Neuron* **19**, 995-1005.

Kolodkin, A. L., Levengood, D. V., Rowe, E. G., Tai, Y. T., Giger, R. J. and Ginty, D. D. (1997). Neuropilin is a semaphorin III receptor. *Cell* **90**, 753-762.

Kubo, H., Fujiwara, T., Jussila, L., Hashi, H., Ogawa, M., Shimizu, K., Awane, M., Sakai, Y., Takabayashi, A., Alitalo, K. et al. (2000). Involvement of vascular endothelial growth factor receptor-3 in maintenance of integrity of endothelial cell lining during tumor angiogenesis. *Blood* **96**, 546-553.

Makinen, T., Jussila, L., Veikkola, T., Karpanen, T., Kettunen, T., Pulkkanen, K. J., Kauppinen, R., Jackson, D. G., Kubo, H., Nishikawa, S. I. et al. (2001). Inhibition of lymphangiogenesis with resulting lymphedema in transgenic mice expressing soluble VEGF receptor-3. *Nat. Med.* **7**, 199-205.

Mandriota, S. J., Jussila, L., Jeltsch, M., Compagni, A., Baetens, D., Prevo, R., Banerji, S., Huarte, J., Montesano, R., Jackson, D. G. et al. (2001). Vascular endothelial growth factor-C-mediated lymphangiogenesis promotes tumor metastasis. *EMBO J.* **20**, 672-682.

Miao, H. Q., Soker, S., Feiner, L., Alonso, J. L., Raper, J. A. and Klagsbrun, M. (1999). Neuropilin-1 mediates collapsin-1/semaphorin III inhibition of endothelial cell motility: functional competition of collapsin-1 and vascular endothelial growth factor. *J. Cell Biol.* **146**, 233-242.

Moyon, D., Pardanaud, L., Yuan, L., Bréant, C. and Eichmann, A. (2001). Plasticity of endothelial cells during arterial-venous differentiation in the avian embryo. *Development* **128**, 3359-3370.

Neufeld, G., Cohen, T., Gengrinovitch, S. and Poltorak, Z. (1999). Vascular endothelial growth factor (VEGF) and its receptors. *FASEB J.* **13**, 9-22.

Neufeld, G., Cohen, T., Shraga, N., Lange, T., Kessler, O. and Herzog, Y. (2002). The neuropilins: multifunctional semaphoring and VEGF receptors that modulate axon guidance and angiogenesis. *Trends Cardiovasc. Med.* **12**, 13-19.

Oh, S. J., Jeltsch, M. M., Birkenhäger, R., McCarthey, J. E. G., Weich, H. A., Christ, B., Alitalo, K. and Wilting, J. (1997). VEGF and VEGF-C: specific induction of angiogenesis and lymphangiogenesis in the differentiated avian chorioallantoic membrane. *Dev. Biol.* **188**, 96-109.

Puri, M. C., Rossant, J., Alitalo, K., Bernstein, A. and Partanen, J. (1995). The receptor tyrosine kinase TIE is required for integrity and survival of vascular endothelial cells. *EMBO J.* **14**, 5884-5891.

Sabin, F. R. (1909). The lymphatic system in human embryos, with a consideration of the system as a whole. *Am. J. Anat.* **9**, 43-91.

Skobe, M., Hawighorst, T., Jackson, D. G., Prevo, R., Janes, L., Velasco, P., Riccardi, P., Alitalo, K., Claffey, K. and Detmar, M. (2001). Induction of tumor lymphangiogenesis by VEGF-C promotes breast cancer metastasis. *Nat. Med.* **7**, 192-198.

Soker, S., Takashima, S., Miao, H. Q., Neufeld, G. and Klagsbrun, M. (1998). Neuropilin-1 is expressed by endothelial and tumor cells as an isoform-specific receptor for vascular endothelial growth factor. *Cell* **92**, 735-745.

Stacker, S. A., Caesar, C., Baldwin, M. E., Thornton, G. E., Williams, R. A., Prevo, R., Jackson, D. G., Nishikawa, S., Kubo, H. and Achen, M. G. (2001). VEGF-D promotes the metastatic spread of tumor cells via the lymphatics. *Nat. Med.* **7**, 186-191.

Stalmans, I., Ng, Y. S., Rohan, R., Fruttiger, M., Bouche, A., Yuce, A., Fujisawa, H., Hermans, B., Shani, M., Jansen. S. et al. (2002). Arteriolar and venular patterning in retinas of mice selectively expressing VEGF isoforms. *J. Clin. Invest*. **109**, 327-336.

Takashima, S., Kitakaze, M., Asakura, M., Asanuma, H., Sanada, S., Tashiro, F., Niwa, H., Miyazaki Ji, J., Hirota, S., Kitamura, Y. et al. (2002). Targeting of both mouse neuropilin-1 and neuropilin-2 genes severely impairs developmental yolk sac and embryonic angiogenesis. *Proc. Natl. Acad. Sci. USA* **99**, 3657-3662.

Veikkola, T., Karkkainen, M., Claesson-Welsh, L. and Alitalo, K. (2000). Regulation of angiogenesis via vascular endothelial growth factor receptors. *Cancer Res.* **60**, 203-212.

Veikkola, T., Jussila, L., Makinen, T., Karpanen, T., Jeltsch, M., Petrova, T. V., Kubo, H., Thurston, G., McDonald, D. M., Achen, M. G. et al. (2001). Signalling via vascular endothelial growth factor receptor-3 is sufficient for lymphangiogenesis in transgenic mice. *EMBO J.* **15**, 1223-1231.

Wigle, J. T. and Oliver, G. (1999). Prox1 function is required for the development of the murine lymphatic system. *Cell* **98**, 769-778.

Wigle, J. T., Harvey, N., Detmar, M., Lagutina, I., Grosveld, G., Gunn, M. D., Jackson, D. G. and Oliver, G. (2002). An essential role for Prox1 in the induction of the lymphatic endothelial cell phenotype. *EMBO J.* **21,** 1505-1513.

Wilting, J., Birkenhäger, R., Eichmann, A., Kurz, H., Martiny-Baron, G., Marmé, D., McCarthy, J., Christ, B. and Weich, H. (1996). VEGF 121 induces proliferation of vascular endothelial cells and expression of flk-1 without affecting lymphatic vessels of the chorioallantoic membrane. *Dev. Biol.* **176**, 76-85.

Wilting, J., Eichmann, A. and Christ, B. (1997). The avian VEGF receptor homologues Quek1 and Quek2 in blood-vascular and lymphatic endothelial and non-endothelial cells during quail embryonic development. *Cell. Tissue Res.* **288**, 207-223.

Wilting, J., Papoutsi, M., Schneider, M. and Christ, B. (2000). The lymphatic endothelium of the avian wing is of somitic origin. *Dev. Dyn.* **217**, 271-278.